



Published in final edited form as:

Dev Neurobiol. 2016 December ; 76(12): 1342–1359. doi:10.1002/dneu.22396.

A window into brain development: hdEEG methods to track visual development in non-human primates

Angela C. Voyles¹ and Lynne Kiorpes¹

¹Center for Neural Science, New York University

Abstract

Background—Electroencephalography (EEG) is widely used to study human brain activity, and is a useful tool for bridging the gap between invasive neural recording assays and behavioral data. We adapted high-density EEG (hdEEG) methods currently used for human subjects for use with infant macaque monkeys, a species that exhibits similar visual development to humans over a shorter time course. Unlike monkeys, human subjects are difficult to study longitudinally and are not appropriate for direct within-species comparison to neuronal data.

New Methods—We designed 27-channel electrode caps, which allowed collection of hdEEG data from infant monkeys across development. We obtained acuity and contrast sweep VEP responses to grating stimuli and established a new method for objective threshold estimation based on response signal-to-noise ratios at different stimulus levels.

Results—We compared the developmental trajectories of VEP-measured contrast sensitivity and acuity to previously collected behavioral and neuronal data. Our VEP measures showed similar rates of development to behavioral measures, both of which were slower than direct neuronal measures; VEP thresholds were higher than other measures.

Comparison with Existing Method(s)—Ours is the first use of this non-invasive technology in non-human primates. Other means to assess neural sensitivity in infants are all invasive.

Conclusions—Use of hdEEG with infant monkeys opens many possibilities for tracking development of vision and other functions in non-human primates, and can expand our understanding of the relationship between neuronal activity and behavioral capabilities across various sensory and cognitive domains.

Keywords

visual development; spatial vision; hdEEG; macaque monkey; brain development

INTRODUCTION

The process of maturing from an infant into a fully functional adult requires extensive brain development: growth of neurons, formation of new synapses, and removal of those that are unnecessary. Through neural reorganization based on experience, infants eventually learn to move through the world and make sense of their surroundings. Much research is devoted to the endpoint of these changes—the structure and function of the adult brain—yet little is known about the maturation process or the way in which this endpoint is reached.

It is well known that atypical patterns of development can give rise to a diverse range of disorders, from cognitive, such as autism spectrum disorders (ASD), which are associated with irregular connectivity (Courchesne, 2005; for review see Maximo et al., 2014), to sensory, such as amblyopia, which is associated with abnormal binocular input (Kiorpes & Movshon, 2004). Studying these disorders reveals aspects of development that are essential for normal maturation and offers potential targets for future treatment of the disorders. However, it is necessary to understand how typical brain development progresses on both the neural and behavioral levels to fully understand how the process is compromised by abnormalities postnatally.

The visual system provides a good model system for tracking the typical developmental plan on both the neural and behavioral levels. The cortical substrates for basic adult vision are already well-mapped near birth, with cells in primary visual cortex responding to features such as the orientation and contrast of stimuli, and areas organized retinotopically (Wiesel & Hubel, 1974; Blasdel et al., 1995; Horton & Hocking, 1996; Chino et al., 1997; Kiorpes & Movshon, 2004; Zheng et al., 2007). Additionally, developmental trajectories for behavioral measures of basic visual functions have been described in detail in non-human primates: both acuity and contrast sensitivity are measurable near birth and progress steadily to adult levels, asymptoting around 1 year of age in monkeys; these functions reach adult levels sometime between 3 and 7 years of age in humans (Boothe et al., 1988; ElleMBERG et al., 1999; Kiorpes, 1992; Teller, 1997; Stavros & Kiorpes, 2008).

Understanding the many changes that take place as visual capabilities mature requires tracking the full trajectory from infancy to adulthood. This is not a trivial task for human development, which can continue into a subject's teenage years (e.g., Kovács et al., 1999; Bucher et al., 2006). As a result, most studies only sample one or a few select age points, leaving gaps in the literature and a patchy understanding of when various capabilities arise and the subsequent course of maturation (see Nayar et al., 2015). For example, Valenza and colleagues (2011) concluded that human infants were able to perform object completion as newborns. Other groups that studied the development of similar visual mechanisms found that 3-month-old infants were not sensitive enough to perform a contour completion task (Gerhardstein et al., 2004), and that this ability continues to develop up to about 14 years of age (Kovács et al., 1999). As with much of the developmental literature, the time period between infancy and school-age remains mostly untested for object completion, though we know that much visual development is still occurring during this window.

Animal models are useful in addressing these issues in the study of development, in part because their maturation takes place over a shorter time frame. Development of spatial vision in macaque monkeys, for example, occurs at a rate that is approximately four times as fast as in humans (Teller & Boothe, 1979), making it feasible to longitudinally track changes over the entire period of interest and avoid the age gaps found in much of the human literature.

In addition to their faster time course, an animal model affords the opportunity to directly relate behavioral and actual neural assays of development. To fully understand the mechanisms of visual development, we must be able to compare changes in behavior with

those in the underlying neural activity. Due to the invasive nature of in vivo cellular recordings, studies of human development cannot directly examine the activity of single neurons or their interconnections. For the neural data from animal models to translate to an understanding of human development, a method to bridge across species is essential.

Electroencephalographic (EEG) technology is well-suited to bridge this gap. The non-invasive nature of the technique allows for repeated testing throughout infancy and childhood; the behaviors required are simple enough even for young infants. Visual evoked potentials (VEPs) make use of repeated stimuli so that EEG responses can be averaged over multiple trials for a rapid assessment of visual function (e.g., Norcia, 1990; Norcia et al., 2005; Gilmore et al., 2007). More recently, this technique has been translated to high-density EEG (hdEEG) experiments (e.g., Wattam-Bell et al., 2010; Ales et al., 2012), allowing assessment of evoked potentials at different locations across the scalp, greatly increasing the power and utility of the method. However, hdEEG, like other VEP measures, remains an indirect metric for identifying the neural changes underlying visual development without the use of more direct neural recording. We sought to develop these methods for use with macaque monkeys so that hdEEG data can be correlated with directly-measured neural changes as well as related to behaviorally-measured visual development. Our understanding of this relationship can then be extrapolated to studies of human infants.

To these ends, we developed a novel method for reliable measurement of longitudinal visual sensitivity using hdEEG in infant macaque monkeys and an analysis approach that reduces the potential for including noisy data and human error. To validate the techniques, we measured contrast sensitivity and spatial acuity development with steady-state VEP methods at multiple sites across the scalp, and compared the trajectories with behavioral and neural data from the same species. We found VEP developmental trajectories obtained with our new threshold evaluation approach to be comparable to those obtained behaviorally, and in line with those obtained by more standard methods used with humans.

Additionally, the hdEEG methodology allowed us to examine the development of signals recorded from electrodes across the whole scalp, confirming our expectations of finding the strongest and earliest developing signals on channels that are in closest proximity to primary visual cortex. In the future, however, this methodology can be used to explore the patterns of activity elicited by higher order stimuli that may activate entirely different areas of the brain.

METHODS

Subjects

Subjects were 5 visually normal pig-tailed macaque monkeys (*Macaca nemestrina*; 3 males, 2 females) between the ages of 5 and 160 weeks. All but one animal was born at New York University. The other animal was born at the University of Washington and transported to our nursery at an appropriate age. All animals were tested multiple times throughout development. Infants were housed in cages enriched with food and toys and were given opportunities to socialize with humans and other monkeys daily. All experiments took place under protocols complying with the NIH Guide for the Care and Use of Laboratory Animals and approved by the New York University UAWC.

Stimuli

Stimuli were presented on a monochromatic 21-inch monitor (HP model p1230, mean luminance 29.97 cd/m², 1600x1200 pixels, frame rate 60 Hz) and viewed at a distance of 60 cm. Experiments were run with steady-state parameter-swept stimuli that were generated and presented using PowerDiva software (Stanford University).

In each of three stimulus conditions, a contrast-alternating grating (3 Hz) was presented for a duration of 10 seconds per trial. In the first condition, the contrast of a low spatial frequency grating (1 cpd) was reduced in logarithmic steps from 80% to 1.19%. The second condition was the same as the first, but used a higher spatial frequency grating (3 cpd). In the third condition, a grating was swept from low to high spatial frequency (0.50 to 10.47 cpd) at a fixed contrast level of 80%.

Testing environment

During the experiments, subjects passively viewed stimuli from a custom-designed Plexiglas testing chair that exposed only their heads (Figure 1). The height of the chair was adjusted to position the subject at eye-level with the stimulus monitor. A tube was placed at the front of the chair to deliver liquid rewards as needed. Gaze location was manually monitored using an infrared camera affixed to the top of the stimulus monitor and viewed on a separate video monitor placed near the stimulus monitor. This allowed the experimenter to monitor the position of the subject's pupils, which appeared as white circles when they were directly in line with the infrared camera and, thus, the stimulus monitor.

Evoked potential data were collected using custom-made 27-channel electrode caps (EasyCap, GmbH, Herrsching-Breitbrunn, Germany). An example cap is displayed in Figure 2, along with the electrode map. Three sizes of the cap were made so that we could record from animals as young as 5 weeks up to adults; the best-fitting cap was selected for the subject at each session. The electrode layout was the same for all three caps. The material was a medium elasticity fabric with openings for the electrodes (EasyCap B-15, extra small sintered Ag/AgCL). Connection was made to a BrainAmp 32-channel EEG recording system (Brain Vision LLC, Morrisville, NC, USA). Prior to each session, electrodes were prepped with conductive gel (Abralyt HiCl, Brain Vision LLC) until impedance was measured to be lower than 20–40 kOhms by the Brain Vision Recorder software.

Training

Behavioral training began approximately 2 weeks before the start of data collection, at the age of 3 weeks or older. Each subject was incrementally acclimated to the room, then to the chair, and then to the EEG cap that was placed on her head. Throughout the acclimation process, treats (baby food for the youngest, raisins and nuts for the older animals) and liquids (baby formula for the youngest, diluted apple juice after weaning) were provided as positive reward of good behavior. Once she was able to quietly sit in the chair, she was regularly rewarded for sitting for longer periods and looking at the stimulus monitor. Gaze position training was then begun.

Noisemaking toys were used to attract the subject's attention to the stimulus monitor. She was rewarded for looking toward the monitor, and once that was accomplished, for holding her gaze at the center of the screen for multiple seconds at a time, as monitored by the experimenter using the infrared camera, so that full stimulus sweeps could be presented.

High-density VEP experiment

Data collection began once the subject was calm, facing forward, and fixating the screen, and could be paused if a break in fixation occurred. Continued proper fixation was rewarded at random intervals with a small amount of liquid. Following fixation breaks or intertrial pauses, data collection was resumed once the animal returned her eyes to the center of the monitor. 15–20 trials, of duration 10 seconds each, were collected per session. To gather 15–20 trials for each condition, data could be combined over multiple sessions (sometimes over consecutive days); in that case, trials from all sessions that passed artifact rejection (discussed below) were combined before thresholds were calculated.

Data analysis

Data collection occurred at a rate of 5000 Hz with Brain Vision Recorder software and amplified using the Brain Amp Standard (Brain Vision LLC). After completion of an experiment, recordings were imported into PowerDiva at a sampling rate of 300.52 Hz and filtered with 200 microvolt artifact rejection.

Thresholds from the sweep VEPs were obtained in two ways: the standard method originally developed by Norcia and Tyler (1985), and a novel adaptation that we developed to enhance reliability of estimation and reduce the influence of noisy channels. For the standard method, neural responses are averaged across trials at each “step” of the stimulus sweep: contrast level (for conditions 1 and 2) or spatial frequency (for condition 3). The averaged response waveform at a given step was then analyzed in the Fourier domain, resulting in an amplitude and phase response for each step (see Figure 3). For threshold evaluation, responses are analyzed at a relevant frequency. Due to the nature of our stimulus design, information about changes in the stimulus is carried by the even harmonics of the stimulus presentation frequency (6 Hz, 12 Hz, etc.), and so responses were analyzed at these frequencies. The responses are processed with a two-weight adaptive filter that takes into account both amplitude and phase in generating VEP responses (Tang & Norcia, 1995). From these responses, the point of highest amplitude that satisfies phase and SNR requirements is identified, and a linear regression is fit to the data between it and the point at which the signal dips below the noise (calculated as the average amplitude of the flanking frequencies, which are 5.5 and 6.5 Hz for analysis of the 2F, or 6 Hz, response). Figure 4 illustrates this standard method of threshold evaluation. A linear regression is fit between the two points marked with arrows, and threshold is taken as the point at which this linear regression reaches an amplitude of zero. We performed this standard analysis of our data for three different harmonics of the stimulus presentation frequency of 3 Hz: 2F (6 Hz), 4F (12 Hz), and 6F (18 Hz).

Without taking into account both phase and amplitude, sweep VEP plots would be noisy, with responses that are not in phase with other signals still possibly contributing non-zero

amplitudes to the data set. This is evident when plotting responses for a given electrode as vectors in the complex plane (see Figure 5, top). In these figures, the direction of the vector indicates the phase of the response, and the length of the vector indicates the amplitude of the response. The shades of grey indicate different steps of the sweep. Higher contrasts and lower spatial frequencies (stimuli that should produce stronger, more reliable responses) are depicted in dark grey. As the contrast decreases or spatial frequency increases, the shade of the vector becomes lighter. The raw amplitude and phase for each stimulus step is also plotted (Figure 5, middle and bottom, respectively).

The standard method of VEP threshold evaluation relies on an adaptive filter to simultaneously account for the phase and amplitude of VEP responses. We took both phase and amplitude into account in a different way, by projecting our responses onto a reference phase that indicates the phase of a reliable response. We tested a variety of phases to be used as our reference phase: the phase of VEP response to the first step of the sweep (the highest contrast or lowest spatial frequency), the phase of the response with the largest amplitude, and the average phase across all responses. These attempts failed to reduce noise in the VEP sweep response. We were, however, able to obtain reliable fits across data sets by projecting onto the phase of the vector average of the responses to the top three steps of the sweep. In Figure 5, which depicts data collected from a subject at one age in response to the three different conditions, the vector average phase is plotted as a dashed line, and was later used to evaluate the reference phase for each condition in our new method of threshold estimation.

To ensure that we would not be biasing our analysis with a phase that changed with development, we plotted in Figure 6 the phase of the vector average for each subject and channel, averaged over all trials, as a function of the subject's age. Because this reference phase does not appear to change systematically with age, we established that we could select the grand mean average phase across all subjects and channels to be used as a single reference phase for all responses within a single condition, rather than selecting a new reference phase for each response, thus imposing a consistent, reliable analysis structure.

VEP responses were then analyzed by projecting the response vector for each step in the sweep onto the reference phase, producing a new amplitude value. These values were normalized by the standard deviation of the noise at each step, and plotted as signal-to-noise ratio (SNR) as a function of condition parameter. Example fits for single conditions are shown in Figure 7. These resulting curves can be compared to the scalar amplitude and phase plots presented in Figure 5 (middle and bottom panels), obtained from the same data.

Contrast response curves for each channel were fit with second order Michaelis-Menton functions ($S = S_{\max}[A^2/(A^2+C^2)]$), with S being equal to the fit SNR and A the contrast level, with free parameters S_{\max} and C . (e.g., El-Shamayleh et al., 2010). Spatial frequency response curves were fit with exponential functions ($S = S_{\max}[1/e^{(B*A)^2}]$), in which A is now equal to the spatial frequency of the stimulus, and free parameters are S_{\max} and B . "Thresholds" for all conditions were obtained at the point at which SNR was equal to 0.1. Resulting plots were evaluated for goodness of fit with R-squared values. Fits with negative R-squared values (indicating inappropriate use of the fit) or with R-squared values less than

0.25 were excluded from data analysis. These exclusions were rare, less than 4% of the data, for visually-modulated channels.

Developmental trajectories

Threshold measures were averaged across the 8 most posterior electrodes, which lie directly atop occipital cortex and consistently record strong responses to grating stimuli. Average responses from these 8 electrodes were plotted as a function of age to obtain developmental trajectories for the different visual functions tested. These developmental trajectories were then fit with Michaelis-Menten functions with an exponent of 2 (as described above).

RESULTS

Longitudinal data

Developmental trajectories for the visual functions tested show a general increase in sensitivity with age, with some individual differences. Figure 8 depicts the longitudinal acuity and contrast sensitivity data for two subjects. The contrast sensitivities in these cases are from gratings of 3 cpd. This contrast sensitivity measure does not change appreciably in the period tested, suggesting that they may mature earlier than the first test ages. Acuity measures, on the other hand, show increased sensitivity over the period of testing.

Old versus new threshold evaluation method

Past studies using sweep VEPs employed a standard method of threshold evaluation that was originally developed by Norcia and Tyler (1985) (see Methods). Thresholds estimated using this method are selected based on the best (lowest contrast threshold or highest acuity) threshold of any of the electrode channels recorded on a given trial. For our new analysis method, we made two changes to the standard method: in threshold evaluation and in threshold reporting. In threshold evaluation, we projected sweep responses onto a reference phase, fit the resulting responses with Michaelis-Menton functions, and called the response at an arbitrary, low SNR “threshold.” The standard method did not use this projection technique. In the reporting of our thresholds, we took threshold values from each responsive electrode and averaged them to obtain our overall threshold for a subject at a given age, whereas the standard method of threshold reporting was to report only the best threshold.

To compare our new method to the standard method on those two different dimensions, we first compared the methods of threshold *reporting*. We took the thresholds found with our new evaluation method and reported them in both by estimating threshold only from the electrode with the best response and by averaging across all active electrodes, and compared the resulting developmental trajectories. Figure 9 (left column) depicts the cross-sectional data, evaluated with average threshold and best threshold methods, as a function of age.

Figure 9 (right column) depicts a direct comparison of these two methods of threshold reporting. This comparison shows strong linear correlations between the two methods, as expected (for the acuity condition, $R = 0.982$, $p < 0.05$; for low spatial frequency contrast sweep, $R = 0.971$, $p < 0.05$; for high spatial frequency contrast sweep ($R = 0.919$, $p < .05$), by Pearson’s linear correlation).

We then compared the new and standard methods of threshold *evaluation*. We found thresholds for each subject and each electrode using both methods: projecting onto a reference phase and reporting the response at a low SNR, and the standard method of fitting a linear regression according to the Norcia & Tyler (1985) model. In this case, for each subject at each age, we reported the threshold as the average of all active electrodes, regardless of whether those thresholds were obtained by the standard method or the new method.

The comparison of these measures is shown in Figure 10. For acuity and low spatial frequency contrast sensitivity, the standard and new threshold measures were positively correlated with each other. For low spatial frequency contrast sensitivity, there was a strong correlation across methods ($R = 0.876$, $p = .0221$, by Pearson's linear correlation). Acuity measures were well-fit with Michaelis-Menton functions, but were less well correlated across the two methods ($R = 0.385$, $p = 0.115$). High spatial frequency contrast sensitivity computed with the new method as a function of age could not be reliably fit with Michaelis-Menton functions, indicating that this metric does not show a clear developmental trajectory, therefore the standard and new measures were not well correlated in this case ($R = -0.150$, $p = 0.566$). Note that the range of error is greater for the standard method than for our new method confirming that we were successful in improving the reliability of the fits and our estimation of thresholds.

Cross-species comparison to previous VEP studies

Previous non-invasive VEP studies in primates have been conducted exclusively in human infants. Some of these studies evaluated developmental trajectories for visual functions such as acuity and contrast sensitivity (Norcia & Tyler, 1985; Norcia et al., 1990; Allen et al., 1996; Sokol et al., 1992; Auestad et al., 1997), and so can be used as a cross-species reference for the trajectories we evaluated in monkeys.

Figure 11 shows a comparison of human VEP acuity measures collected from previous studies (adapted from Norcia, 2015) and monkey VEP acuity measures from the present study. For ease of comparison across species, all VEP measures were reported as “best” acuity across evaluated electrodes in this case. Human data are plotted in months, while monkey data are plotted in weeks, based on the previously established 4:1 species difference in rates of visual development (Teller & Boothe, 1979). As translated by this metric, within the range of overlapping age, monkey acuity was similar to human acuity, although it is difficult to compare the youngest and oldest ends of the age range because of a lack of overlap in data at those ages.

Comparison to behavioral and neuronal data

VEP data for all animals tested, cross-sectional as well as longitudinal, are plotted in Figure 12. Acuity measures for the group (5 subjects) are shown in Figure 12A (black symbols) in comparison with developmental responses measured by other methods. Behavioral acuity data (open symbols) were collected from previous experiments conducted by Kiorpes and colleagues that utilized two-alternative forced-choice (2-AFC) psychophysics to evaluate

monkeys' acuity and contrast sensitivity throughout development (Movshon & Kiorpes, 1988; Boothe et al., 1988; Kiorpes, 1992).

Neuronal data (filled grey symbols) were collected from single-cell recordings in area V1 of the same species of macaque (Movshon et al., 1999; Movshon et al., 2000; see Kiorpes and Movshon, 2004). These thresholds were estimated from the geometric mean of the resolution limit for populations of recorded neurons. While they do not reflect actual acuity measures, they are good approximations for the spatial resolution of the population of V1 cells at each age tested.

Our VEP measures of acuity result in higher thresholds than those obtained by behavioral and neuronal measures, but the developmental trajectories for behavior and VEP are similar. Neither behavioral nor VEP measures were able to approximate the high acuity indicated by neuronal measures at the youngest ages.

The full data sets for the contrast sweep conditions are shown in Figure 12B and C. In the low spatial frequency contrast sweep condition (Figure 12C), the trajectory of VEP sensitivity closely mirrors the behavioral contrast sensitivity trajectory, with similar slopes and overlapping sensitivities. VEP sensitivity to the high spatial frequency contrast sweep condition (Figure 12B) does not show a consistent developmental trend, but the data sets do largely overlap. Because neuronal contrast sensitivity is measured at the preferred spatial frequency for each neuron, rather than at a consistent SF, we do not have comparable neuronal data sets for these conditions.

Evaluation of sensitivity by channel

To explore the benefit of the high-density EEG recordings, we evaluated the developmental trajectories of contrast sensitivity and acuity for each electrode across the scalp. In these analyses, data points indicate that thresholds could be obtained from the VEP sweeps evaluated at a given harmonic. If no threshold could be obtained—either due to poor signal quality or a lack of amplitude modulation with the swept stimulus parameters—then no data point was plotted for that electrode for that subject at that age.

Figure 13A depicts these trajectories for acuity development as measured from the 2F harmonic response. The occipital channels show the clearest trend of increasing sensitivity, which supports our use of these channels in our initial averaged analyses, but interestingly, some more forward and lateral channels also show clear patterns of improved acuity with age.

Figures 13B–C show developmental trajectories for contrast sensitivity measured with 1 and 3 cpd gratings, also at the 2F harmonic. Again, occipital and lateral electrodes show the strongest trends. Consistent trends are less clear for higher spatial frequency contrast sensitivity.

We also examined developmental trajectories for responses at higher harmonics (4F and 6F) to see if different electrodes showed better responses to higher frequencies (data not shown). Responses were much weaker across all electrodes at the higher harmonics, suggesting that the use of the 2F harmonic to evaluate developmental trajectories was most appropriate.

Evaluation of sensitivity by scalp region

One concern of this analysis is that different electrodes will fall on slightly different areas of the scalp for each individual and at each age. To address this, we divided the electrodes into seven different scalp regions, which are more likely to remain consistent even as the head grows with age, and evaluated how sensitivity in these regions changed for a single subject in response to the acuity experiment and the contrast sensitivity experiment (at high spatial frequency). For each condition, the longitudinal profile from a single animal was obtained for each electrode location (rather than as an average of a select group of occipital electrodes), and fit with a Michaelis-Menton function. This particular animal, B6, was chosen as an example because of the broad age range of testing that she underwent, ensuring more complete developmental profiles. From this fit, the resulting maximum sensitivity (S_{\max}) and age at which half maximum sensitivity was reached (C) were then evaluated as a function of electrode location, anterior to posterior, with the occipital electrodes where we expect most activity to take place including regions 5, 6, and 7 (Figure 14A).

Both high spatial frequency contrast sensitivity and acuity measures show an increase in maximum sensitivity (Figure 14B,C) and a decrease in the age at which half maximum sensitivity was reached (Figure 14D,E) as we move from anterior to posterior channels, confirming that the occipital channels that we had previously flagged are contributing the most sensitive responses. Additionally, this suggests that the most posterior channels develop their responses at an earlier age than other channels. When the same analysis was performed for the trajectories of all animals tested, similar results were obtained.

DISCUSSION

VEP measurements of acuity and contrast sensitivity are effective clinical techniques for diagnosing visual deficiencies in infants and other special populations, due to the speed with which the data can be collected and the lack of behavioral feedback required. Due to their widespread use, assessing thresholds with the lowest amount of human error and uncertainty is of practical importance. On a broader scale, it is essential to understand what these thresholds represent: how does a VEP measure relate to an individual's behavioral capabilities and underlying neural function, and where does that measure fall in the context of typical development?

VEP thresholds measured with low-density scalp electrodes in human infants have historically, though not always, shown an earlier maturation of responses than is seen with behavioral measures (Teller, 1997; Skoczenski & Norcia, 2002). We were unable to tell if our monkey VEP thresholds showed consistently earlier maturation of responses than those measured behaviorally due to the lack of VEP data at very young ages. Our data show VEP acuity and contrast sensitivities to be lower on balance, but to develop over similar trajectories compared with behavioral measures. This absolute difference may be due to our use of the average sensitivity across a number of electrodes or to our new methods for exclusion of noisy or random, large evoked activity. It may also reflect our choice of metric for evaluation of threshold at a fixed SNR (0.1).

It is possible that superior sensitivities measured with VEP methods compared with behavior in human infants is due to behavioral methods underestimating visual sensitivity in this population. Motivational issues at the youngest ages might have artificially decreased behavioral sensitivity and steepened the developmental trajectories in those studies. Typically preferential looking is used for infants who cannot emit an operant response to make their selection, but PL still demands a high level of focus from an infant, which may worsen performance if he or she is not engaged or alert. The operant testing and reinforcement techniques used in our lab, however, motivate the infant monkeys and ensure better attention is being paid to the task. This makes it unlikely that our subjects' behavioral sensitivities were underestimated.

Although we were able to obtain VEP measures as young as 5 weeks, we do not have data at young enough ages to make a strong claim as to whether our newly obtained VEP responses better match the previously recorded neural or behavioral trajectories. While it may be possible to obtain VEP data from the infants at younger ages, for example, by hand-holding the infants, our methods limit the age at which full data sets could be obtained. The limitations arose because we elected to use a chair, and positive reinforcement training, to slowly acclimate the infants to the test environment. This is advantageous for three reasons. First, the infants once trained sit calmly for long periods of time and maintain their gaze on the center of the screen, thus ensuring accurate viewing distance and location of visual stimulation. Secondly, they cannot reach out to access the cap or the wires, and their calm state allows for acquisition of better, more stable signals. Thirdly, by adjusting the cap size and the seat position in the chair, the same protocol can be used throughout at least the first 12–18 months after birth, thus ensuring consistency of data collection across age. As noted above, absolute measures of VEP, behavioral, and neuronal acuity were not directly in line with each other, but trajectories are the important comparison, and they were similar across the range of ages that we tested.

New Threshold Estimation

Our new method of analysis, which takes into account both the amplitude and the phase of the VEP response, removes noise that might be included when a response component has a large amplitude but is out of phase with the true responses. It also eliminates any bias that might occur during standard threshold estimation when determining the best linear fit for threshold extrapolation or selecting the best channel. Averaging across all responsive channels takes account of all the available information. The resulting sensitivity measures at low SF and for acuity, were correlated with the standard method as well as with behavior, which suggests that our method is both valid and useful. The lack of a clear correlation between methods for the higher SF data set may be due to noisier or less reliable signals at that spatial-temporal frequency combination (see below). Comparison of the error estimates for the two analysis methods shows that our phase-adjusted method of evaluation substantially improved the reliability of our fits.

Our resulting measurements show lower sensitivities in general than the traditional threshold evaluation method, yielding somewhat lower acuities and lower contrast sensitivity measures in some cases. However, this is most likely primarily due to differences in where we chose to

set threshold. Norcia and colleagues fit a linear regression to the falling portion of the sweep and extrapolate the fit to an amplitude of zero, while we fit an exponential function and selected a particular y-value (SNR = 0.1) as our threshold. We would not expect these values to be exactly equivalent, but the strong correlations and similar rates of change with development suggest that they are related as they should be.

We found it puzzling that the 3 cpd data did not consistently reflect development over the age range we tested but the lower spatial frequency did show development. While one might conclude that sensitivity does not change beyond the early postnatal weeks at this frequency, this seems at odds with ample behavioral data showing in fact greater increase in sensitivity at 3 cpd compared to lower spatial frequencies in infant monkeys as a function of age (Boothe et al., 1988; Movshon & Kiorpes, 1988; Kiorpes & Kiper, 1996). In human adults, there is an interaction between spatial and temporal contrast sensitivity (e.g. Robson, 1966). The full extent of spatio-temporal interactions has never been measured in developing primates, however, there are hints that even across relatively low spatial frequencies, there are different developmental trajectories at a given temporal frequency in human infants (Moskowitz & Sokol, 1980; Swanson & Birch, 1990). None of the data in the literature included spatial frequencies above 1 cpd, although Moskowitz & Sokol (1980) noted a very different profile for checkerboards with small (12') vs large (48') check sizes. Therefore, it is possible that the two spatial frequencies we chose develop somewhat differently at the temporal frequency we used (3Hz). So, while we found reasonably comparable trajectories between behavior and VEP assessments, this raises a caution that the spatio-temporal nature of the VEP stimulus may not reflect the sensitivity of the same mechanisms as the behavioral data, which are typically collected with static stimuli. To resolve this question, it will be necessary to use a variety of temporal frequencies or even map the full spatio-temporal surface across development.

Benefits of hdEEG

In addition to validating these methods in an animal model and establishing a new method of threshold estimation, we sought to explore the benefits offered by high-density EEG in infant monkeys. Practically speaking, the use of a high-density EEG cap improved electrode contact, stabilization, and consistency in location of placement over the use of single, individually placed electrodes. Our method also allowed us to examine developmental trajectories for each individual electrode at many locations across the scalp. In doing this, we found that the eight occipital channels that we had originally pre-selected as being the most responsive, due to their close proximity to primary visual cortex, did show the most sensitive responses to our grating stimuli, as well as earlier development of those responses. Some electrodes on more anterior regions of the scalp also reflected increased acuity and contrast sensitivity with age, but those locations were less consistently active. Averaging over scalp regions for a single, longitudinally tested animal showed a strong trend of posterior scalp regions producing the strongest responses at the earliest age.

We also analyzed responses to different harmonics of the stimulus. While the strongest responses were found at the second harmonic response of the stimulus presentation (6 Hz) frequency, we posited that more anterior channels may show stronger responses at other

harmonics of the stimulus presentation (12 Hz, 18 Hz, etc.), and more information may be present there. However, we did not find this to be the case: responses across the scalp were weaker at the higher harmonics, leading to less easily obtained thresholds. As a result, developmental trends were much less consistent at the higher harmonics.

CONCLUSIONS

The hdEEG technique can provide insight into the timing of development, which correlates with behavioral trajectories, but lags behind directly-measured assays of neural development. The poorer measured sensitivity with the VEP compared with single-unit physiology may be because neural sensitivity is measured under optimized conditions for each cell, while the VEP is a reflection of population activity to general grating stimulation. Thus, it appears that the VEP is a good proxy for behaviorally measured sensitivity in monkeys, but should be considered a conservative estimate of neural sensitivity.

hdEEG data reflect the scalp distribution of underlying neural population activity, but it is unclear precisely which brain areas are the source of the signals. Source localization analysis will be necessary to identify the specific visual areas involved in producing these changing responses during development. Based on scalp activity alone, it would be impossible to pinpoint the sources of activity (primary versus secondary visual cortex, for example) or assert with certainty that change or reorganization of any particular cortical mechanism is occurring (Wattam-Bell et al., 2010). This could be accomplished by pairing the VEP responses with structural MRI data obtained from the same individual infants. Recent improvements in techniques have allowed researchers to perform source localization on younger subjects more accurately, using more realistic head models and MRI data for each subject (Ortiz-Mantilla et al., 2012). Still, it is difficult to accomplish this longitudinally in individual human infants, where the frequency of testing is limited. One additional benefit of our study with the nonhuman primate model is that images for each infant monkey can be obtained at regular intervals, allowing for appropriate source localization parameters to be applied throughout development.

The current study provides a novel approach to measure thresholds from VEPs, and establishes this method as a valid way to evaluate the trajectory of visual functions. Additionally, we have provided a within-species comparison to behavioral capabilities and directly-measured neural responses, giving us a better understanding of how visual development progresses on multiple levels. Moving forward, the technique of hdEEG will allow us to investigate whether the development of more complex visual functions, such as contour integration or texture perception, is mediated by similar or distinct neural processes, and opens the possibility of evaluating more cognitive capabilities in the future.

Acknowledgments

This study was supported by NIH grants R21 EY021894 and R01EY05864. The authors would like to thank Anthony M. Norcia, Vladimir Vildavski, David Heeger and J. Anthony Movshon for consultation on this project; Michael Gorman, Solmaz Shariat Torbaghan, Alisa Liu, and Priyanka Ramesh for help with data collection; and Chao Tang for technical assistance. We also thank Matthias Munk for assistance with recording cap design.

References

- Ales JM, Farzin F, Rossion B, Norcia AM. An objective method for measuring face detection thresholds using the sweep steady-state visual evoked response. *Journal of Vision*. 2012; 12(10):18, 1–18.
- Allen D, Tyler CW, Norcia AM. Development of grating acuity and contrast sensitivity in the central and peripheral visual field of the human infant. *Vision Research*. 1996; 36:1945–1953. [PubMed: 8759434]
- Auestad N, Montalto MB, Hall RT, Fitzgerald KM, Wheeler RE, Connor WE, Neuringer M, Connor SL, Taylor JA, Hartmann EE. Visual acuity, erythrocyte fatty acid composition, and growth in term infants fed formulas with long chain polyunsaturated fatty acids for one year. *Ross Pediatric Lipid Study*. *Pediatric Research*. 1997; 41:1–10. [PubMed: 8979282]
- Baldwin MK, Kaskan PM, Zhang B, Chino YM, Kaas JH. Cortical and subcortical connections of V1 and V2 in early postnatal macaque monkeys. *Journal of Comparative Neurology*. 2012; 520:544–569. [PubMed: 21800316]
- Batardière A, Barone P, Knoblauch K, Giroud P, Berland M, Dumas AM, Kennedy H. Early specification of the hierarchical organization of visual cortical areas in the macaque monkey. *Cereb Cortex*. 2002; 12:453–465. [PubMed: 11950763]
- Boothe RG, Kiorpes L, Williams RA, Teller DY. Operant measurements of contrast sensitivity in infant macaque monkeys during normal development. *Vision Research*. 1988; 28:387–396. [PubMed: 3188402]
- Bucher K, Dietrich T, Marcar V, Brem S, Halder P, Boujraf S, ... Loenneker T. Maturation of luminance- and motion-defined form perception beyond adolescence: A combined ERP and fMRI study. *NeuroImage*. 2006:1625–1636. [PubMed: 16624584]
- Callaway EM. Prenatal development of layer-specific local cortical circuits in primary visual cortex of the macaque monkey. *Journal of Neuroscience*. 1998; 18:1505–1527. [PubMed: 9454858]
- Coogan TA, Van Essen DC. Development of connections within and between areas V1 and V2 of macaque monkeys. *J Comp Neurol*. 1996; 372:327–342. [PubMed: 8873864]
- Courchesne E, Pierce K. Why the frontal cortex in autism might be talking only to itself: local over-connectivity but long-distance disconnection. *Current Opinion in Neurobiology*. 2005; 15:225–230. [PubMed: 15831407]
- Ellemborg D, Lewis TL, Liu CH, Maurer D. Development of spatial and temporal vision during childhood. *Vision Research*. 1999; 39:2325–2333. [PubMed: 10367054]
- El-Shamayleh Y, Movshon JA, Kiorpes L. Development of sensitivity to visual texture modulation in macaque monkeys. *Journal of Vision*. 2010; 10:1–12.
- Gerhardstein P, Kovacs I, Ditte J, Feher A. Detection of contour continuity and closure in three-month-olds. *Vision Research*. 2004; 44:2981–2988. [PubMed: 15474571]
- Gilmore RO, Hou C, Pettet MW, Norcia AM. Development of cortical responses to optic flow. *Visual Neuroscience*. 2007; 24:845–856. [PubMed: 18093371]
- Hadad B, Maurer D, Lewis T. The effects of spatial proximity and collinearity on contour integration in adults and children. *Vision Research*. 2010:772–778. [PubMed: 20149911]
- Kennedy, H.; Burkhalter, A. Ontogenesis of cortical connectivity. In: Chalupa, LM.; Werner, JS., editors. *The Visual Neurosciences*. Cambridge, MA: MIT Press; 2004. p. 146-158.
- Kiorpes L. Development of vernier acuity and grating acuity in normally reared monkeys. *Visual Neuroscience*. 1992; 9:243–251. [PubMed: 1390384]
- Kiorpes L, Kiper DC. Development of contrast sensitivity across the visual field in macaque monkeys (*Macaca nemestrina*). *Vision Research*. 1996; 36:239–247. [PubMed: 8594822]
- Kiorpes, L.; Movshon, JA. Neural limitations on visual development in primates. In: Chalupa, L.; Werner, JS., editors. *The Visual Neurosciences*. Cambridge, MA: MIT Press; 2004.
- Kovács I, Kozma P, Fehér A, Benedek G. Late maturation of visual spatial integration in humans. *Proceedings of the National Academy of Sciences of the United States of America*. 1999; 96:12204–12209. [PubMed: 10518600]

- Maximo JO, Cadena EJ, Kana RK. The implications of brain connectivity in the neuropsychology of autism. *Neuropsychology Review*. 2014; 24:16–31. [PubMed: 24496901]
- Moskowitz A, Sokol S. Spatial and temporal interaction of pattern-evoked cortical potentials in human infants. *Vision Research*. 1980; 20:699–707. [PubMed: 7445441]
- Movshon JA, Kiorpes L. Analysis of the development of spatial contrast sensitivity in monkey and human infants. *Journal of the Optical Society of America*. 1988:2166–2166. [PubMed: 3230486]
- Movshon JA, Kiorpes L, Cavanaugh JR, Hawken MJ. Receptive field properties and surround interactions in V1 neurons in infant macaque monkeys. *Neuroscience Abstract*. 1999; 25:1048.
- Movshon JA, Kiorpes L, Cavanaugh JR, Hawken MJ. Developmental reorganization of receptive field surrounds in V1 neurons in macaque monkeys. *Investigative Ophthalmology and Visual Sciences*. 2000; 41(4):333.
- Nayar K, Franchak J, Adolph K, Kiorpes L. From local to global processing: the development of illusory contour perception. *Journal of experimental child psychology*. 2015; 131:38–55. [PubMed: 25514785]
- Norcia AM, Tyler CW. Spatial frequency sweep VEP: visual acuity during the first year of life. *Vision Research*. 1985; 25:1399–1405. [PubMed: 4090273]
- Norcia AM, Tyler CW, Hamer RD, Wesemann W. Measurement of spatial contrast sensitivity with the swept contrast VEP. *Vision Research*. 1989; 29(5):627–637. [PubMed: 2603399]
- Norcia AM, Tyler CW, Hamer RD. Development of contrast sensitivity in the human infant. *Vision Research*. 1990; 30(10):1475–1486. [PubMed: 2247957]
- Norcia AM, Sampath V, Hou C, Pettet MW. Experience-expectant development of contour integration mechanisms in human visual cortex. *Journal of Vision*. 2005; 5:116–130. [PubMed: 15831072]
- Ortiz-Mantilla S, Hamalainen JA, Benasich AA. Time course of ERP generators to syllables in infants: a source localization study using age-appropriate brain templates. *NeuroImage*. 2012; 59:3275–3287. [PubMed: 22155379]
- Robson JG. Spatial and temporal contrast sensitivity functions of the visual system. *Journal of the Optical Society of America*. 1966; 56:1141–1142.
- Skoczenski AM, Brown C, Kiorpes L, Movshon JA. Development of contrast sensitivity and visual efficiency in macaque monkeys measured with sweep VEPs. *Investigative Ophthalmology and Visual Science*. 1995; 36:S442.
- Skoczenski AM, Norcia AM. Development of VEP vernier acuity and grating acuity in human infants. *Investigative Ophthalmology and Visual Science*. 1999; 40:10.
- Skoczenski AM, Norcia AM. Late maturation of visual hyperacuity. *Psychological Science*. 2002; 13(6):537–541. [PubMed: 12430838]
- Sokol S, Moskowitz A, McCormack G. Infant VEP and preferential looking acuity measured with phase alternating gratings. *Investigative Ophthalmology and Visual Science*. 1992; 33:3156–3161. [PubMed: 1399421]
- Stavros KA, Kiorpes L. Behavioral measurement of temporal contrast sensitivity development in macaque monkeys (*Macaca nemestrina*). *Vision Research*. 2008; 48(11):1335–1344. [PubMed: 18406441]
- Swanson WH, Birch EE. Infant spatiotemporal vision: dependence of spatial contrast sensitivity on temporal frequency. *Vision Research*. 1990; 30(7):1033–1048. [PubMed: 2392833]
- Tang Y, Norcia AM. An adaptive filter for steady-state evoked responses. *Electroencephalography and clinical neurophysiology*. 1995; 96:268–277. [PubMed: 7750452]
- Teller DY. First glances: the vision of infants. *The Friedenwald Lectures*. *Investigative Ophthalmology and Visual Science*. 1997; 38(11)
- Teller DY, Boothe RG. Development of vision in infant primates. *Trans Ophthalmol Soc UK*. 1979; 99:333–337. [PubMed: 298809]
- Valenza E, Bulf H. Early development of object unity: evidence for perceptual completion in newborns. *Developmental Science*. 2011; 14(4):799–808. [PubMed: 21676099]
- Wattam-Bell J, Birtles D, Nystrom P, von Hofsten C, Rosander K, Anker S, Atkinson J, Braddick O. Reorganization of global form and motion processing during human development. *Current Biology*. 2010; 20:411–415. [PubMed: 20171101]



Figure 1. EEG test room set-up, including the custom-designed infant monkey chair (*left*), milk/juice dispenser tube (*center*), and stimulus monitor (*right*).

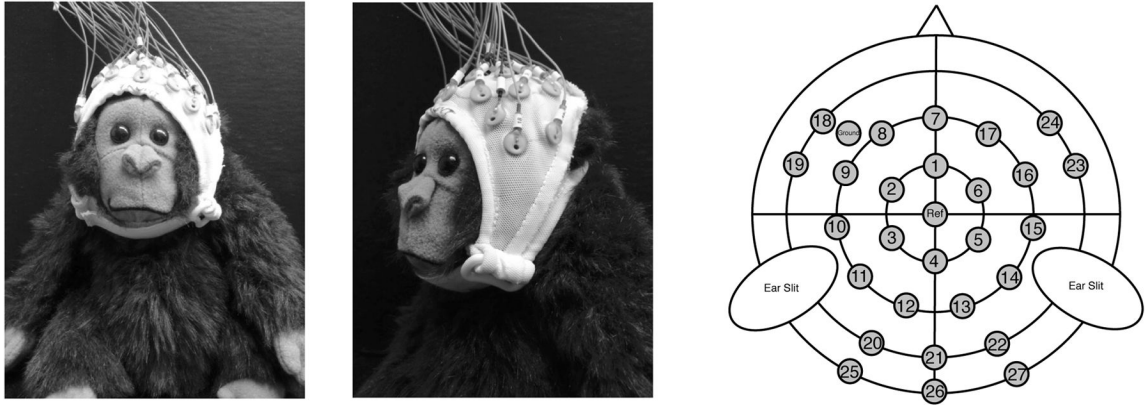


Figure 2. Custom-made 27-channel high-density EEG cap (EasyCap). Cap was created in three sizes (small, medium, and large) to accommodate skull sizes throughout development. The small cap is depicted here, on a model (*left, center*). The layout of all 27 electrodes, reference, and ground can be seen in the schematic of the cap (*right*).

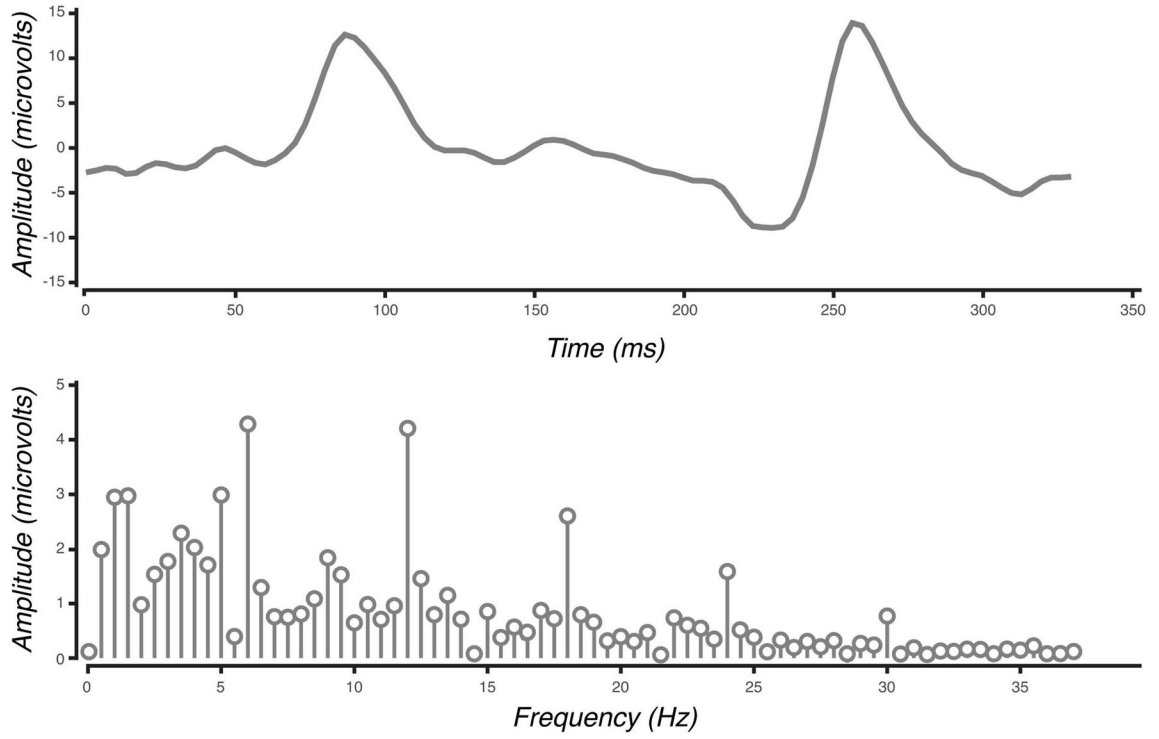


Figure 3. *(Top panel)* VEP waveform from an occipital channel from a single subject in response to the spatial frequency swept stimulus. The waveform is the result of averaging across trials at a single step in the sweep. *(Bottom panel)* The resulting amplitude spectrum from the averaged waveform. Amplitudes were strongest at even harmonics of the stimulus presentation (6 Hz, 12 Hz, 18 Hz, etc.)

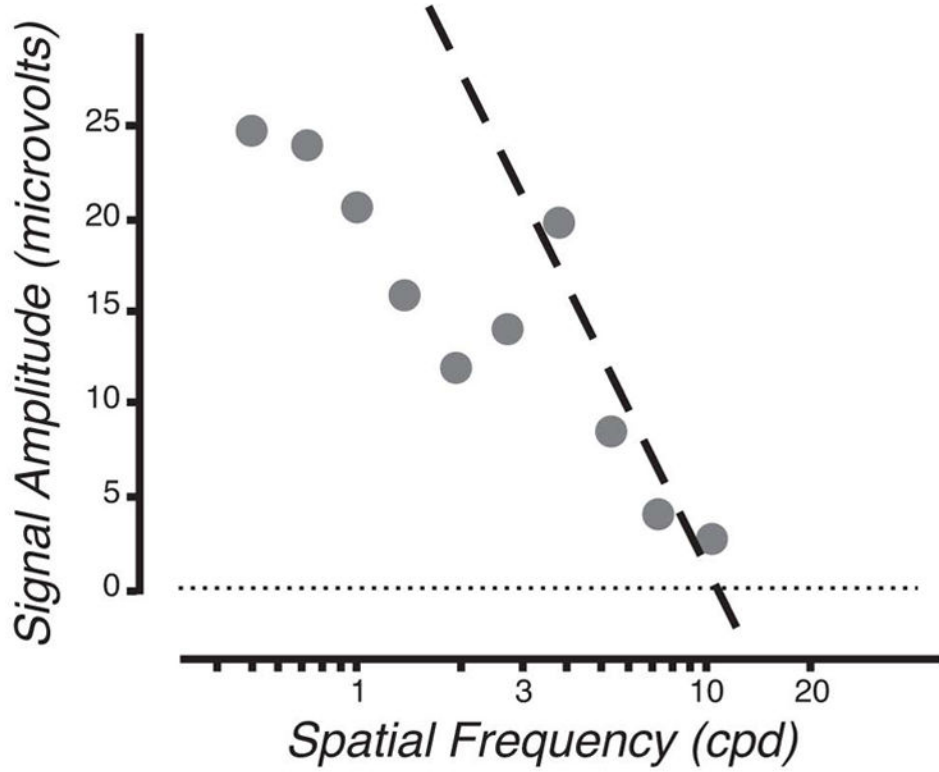


Figure 4. Acuity threshold evaluation for an occipital electrode in the standard method. VEP amplitude at the 2F1 frequency is plotted as a function of spatial frequency. Threshold is determined to be the point at which the linear regression (*dashed line*) reaches an amplitude of zero (*dotted line*).

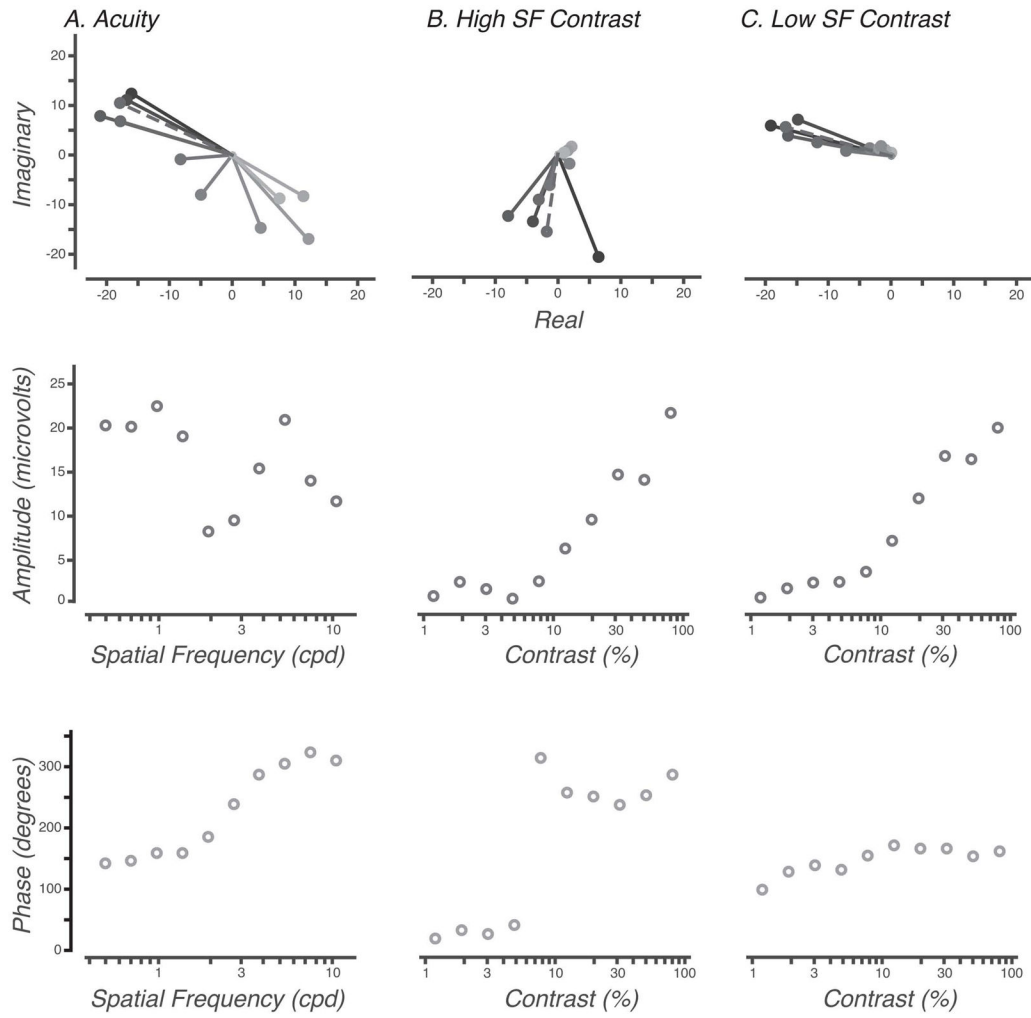


Figure 5. (Top panels) Vector responses to each step of the stimulus sweep are plotted in the complex plane. Dark-grey and black vectors represent early steps of the sweep (low spatial frequency or high contrast gratings), and they become lighter in shade as the sweep progresses. The dashed vector in each frame represents the phase of the vector average of the top three steps, which was later used to evaluate the reference phase. For each condition, we also plotted raw amplitude (middle panels) and phase (bottom panels) as a function of swept stimulus parameter (contrast or spatial frequency).

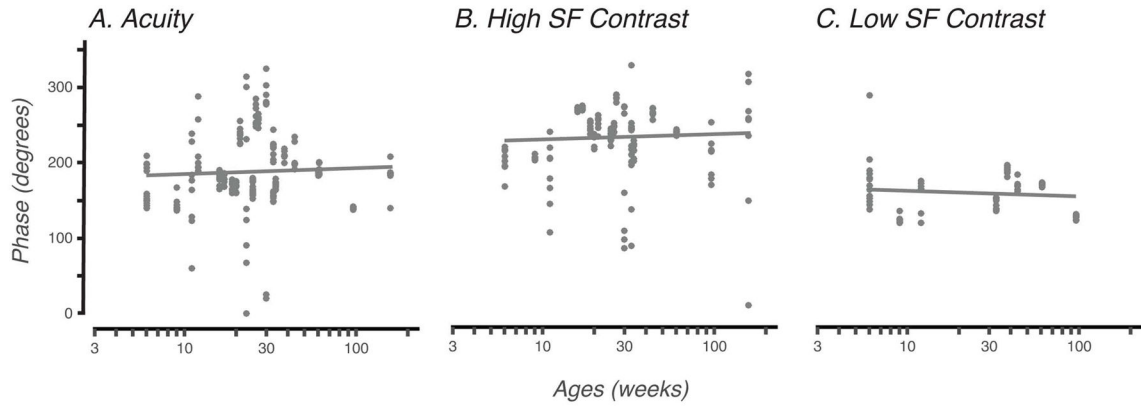


Figure 6. The vector-averaged phase of the VEP sweep (top three steps) was evaluated by condition for each electrode and each subject tested (*grey circles*). These phase values were plotted as a function of age and fit with a linear regression. Since there was no appreciable change taking place with age, we evaluated the grand mean average phase for each condition and used that value as the reference phase in our analyses.

Author Manuscript

Author Manuscript

Author Manuscript

Author Manuscript

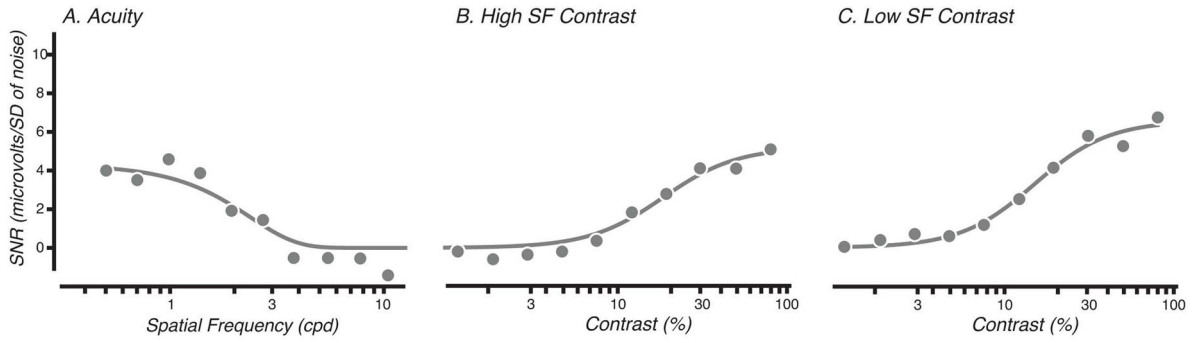


Figure 7. VEP SNR obtained from new analysis methods, plotted as a function of (A) stimulus spatial frequency and fit with a negative exponent function, and (B,C) plotted as a function of stimulus contrast and fit with Michaelis-Menton function. Threshold was obtained at the point in the fit where SNR was equal to 0.1. R-squared values were obtained for the goodness of fit (for acuity, R-squared = 0.747; for high SF contrast, R-squared = 0.964; and for low SF contrast, R-squared = 0.978).

Author Manuscript

Author Manuscript

Author Manuscript

Author Manuscript

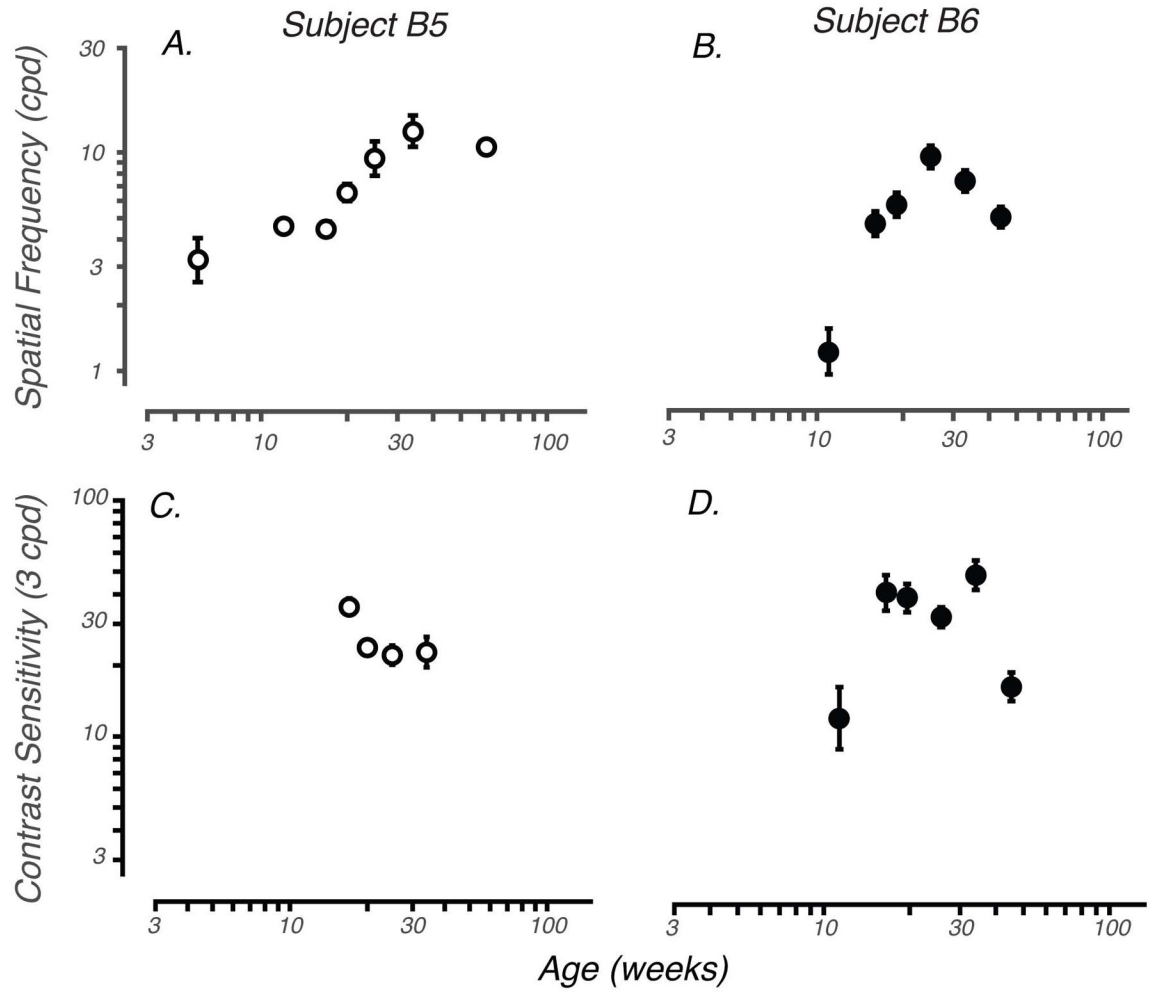


Figure 8. (A–B) Longitudinal development of acuity as measured by VEPs for two individual subjects. Acuity threshold is plotted against age, in weeks, for individual monkeys at several test ages. (C–D) Contrast sensitivity (1/threshold) for 3 cpd gratings is plotted as a function of age for two individual monkeys at several test ages. The contrast sensitivity data for these animals do not change appreciably over the age range tested. Earlier data points for the data sets in panel C were not useable due to technical failure.

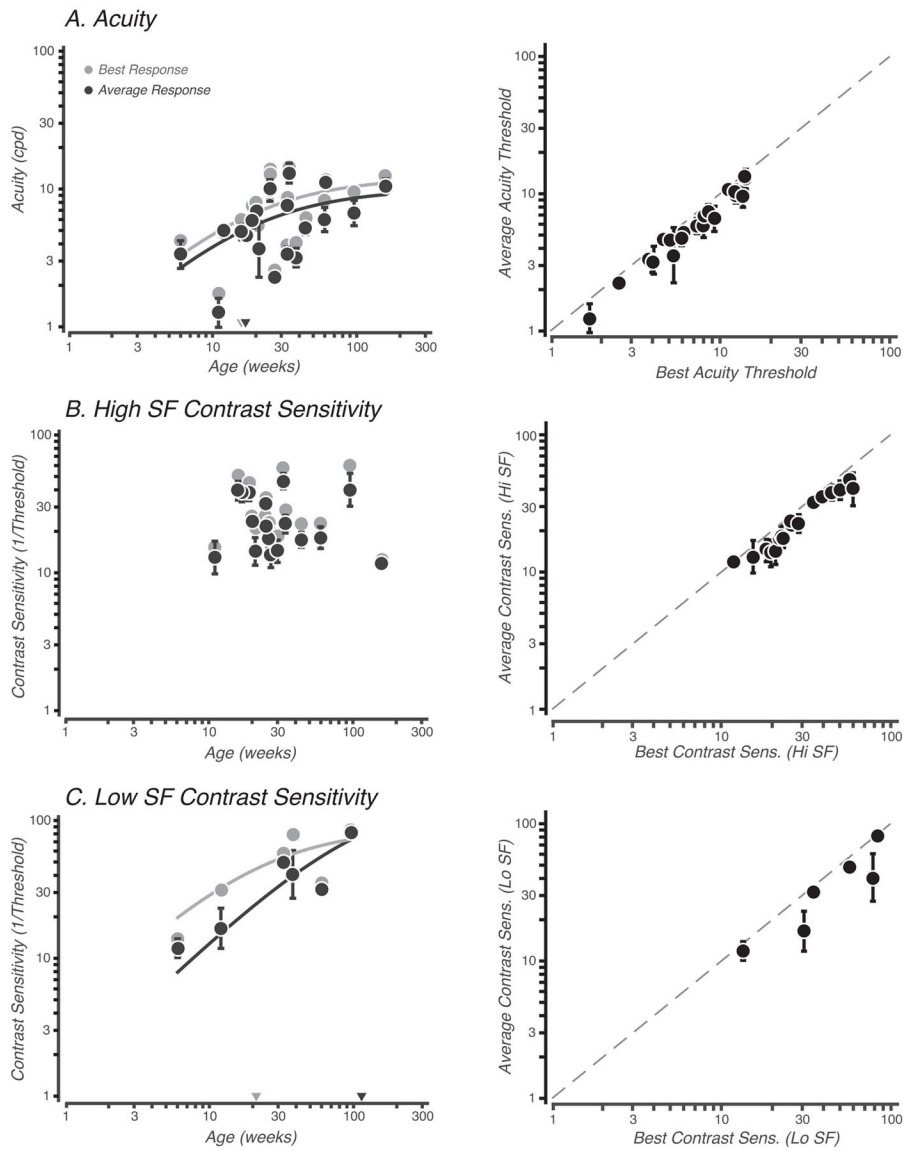


Figure 9. (A, Left) Acuity thresholds plotted as a function of age with two different methods of threshold evaluation: the best acuity threshold (highest spatial frequency) measured on the 8 occipital channels (grey) and the average acuity threshold measured across the 8 occipital channels (black). (A, Right) A direct comparison of thresholds evaluated with the two different measures (grey dashed line represents line of unity). (B,C) The same comparison was done for contrast sensitivity measures. For average threshold measures, error bars indicate the standard error of the threshold estimation. Measures of high spatial frequency contrast sensitivity were not successfully fit with a Michaelis-Menton function.

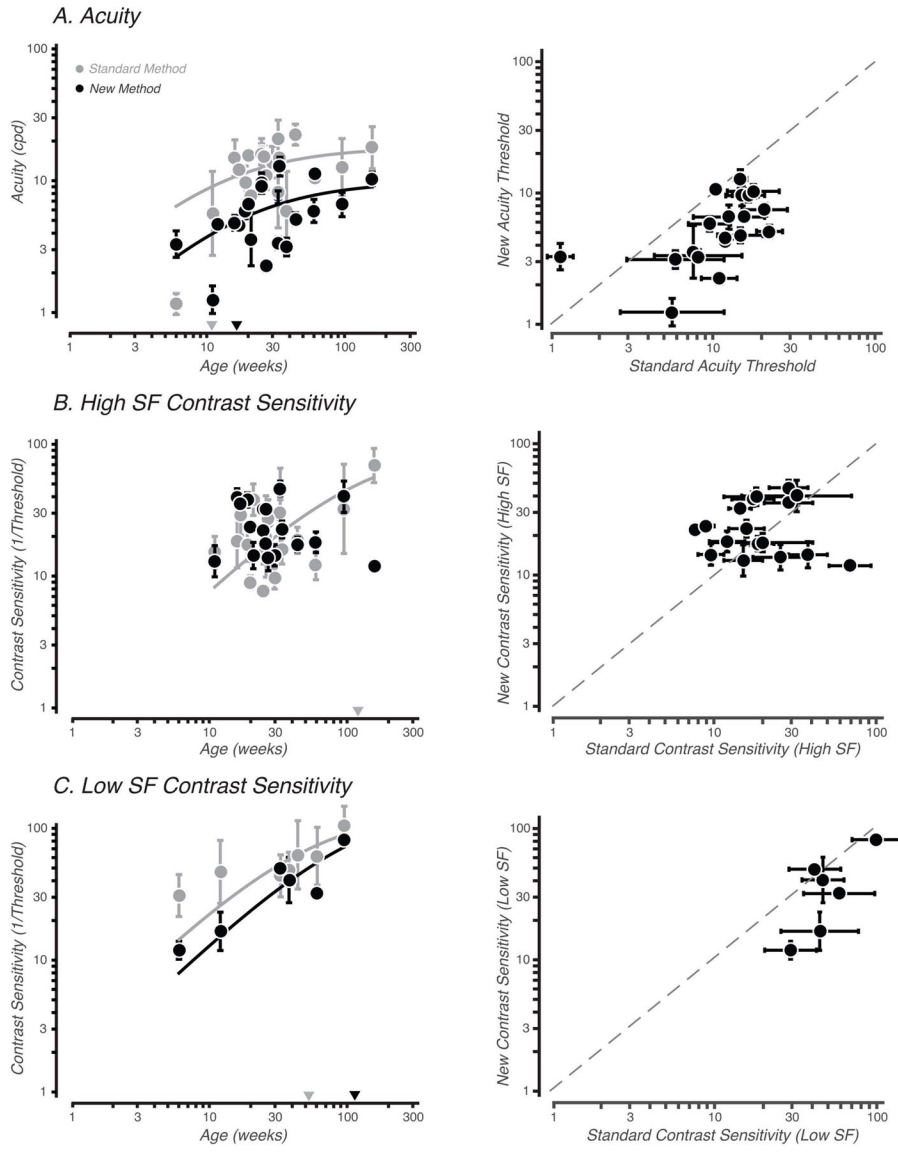


Figure 10. Comparison of results from the standard and new methods of threshold estimation. For each method, the resulting thresholds were averaged over the 8 occipital channels. Error bars indicate the standard errors of the threshold estimation. *Left panels* show the comparison of developmental trajectories from the two methods. *Right panels* show the direct comparison of acuity or contrast sensitivity measures.

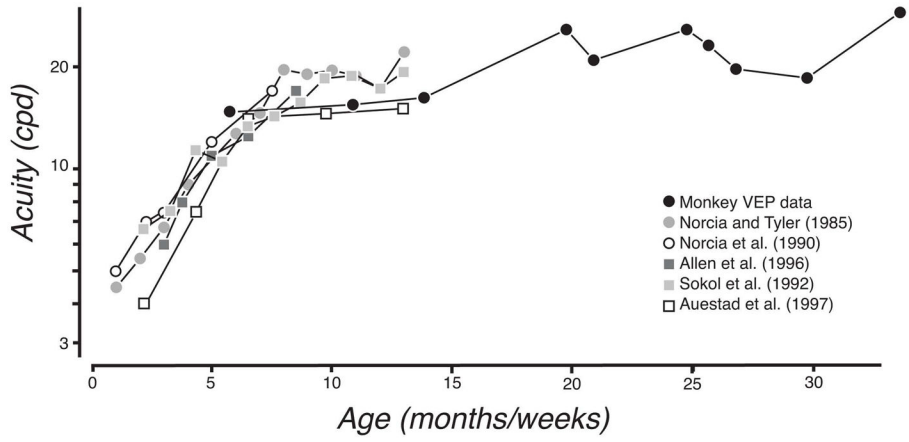


Figure 11. Comparison of VEP acuity development for monkeys (from the present study) and human infants (from previous studies). Age is plotted in weeks for monkeys and in months for humans, based on the 4:1 rate of development previously described. Human VEP acuity data are represented in grayscale symbols, adapted from Norcia (2015). Monkey VEP acuity data are represented with black circles.

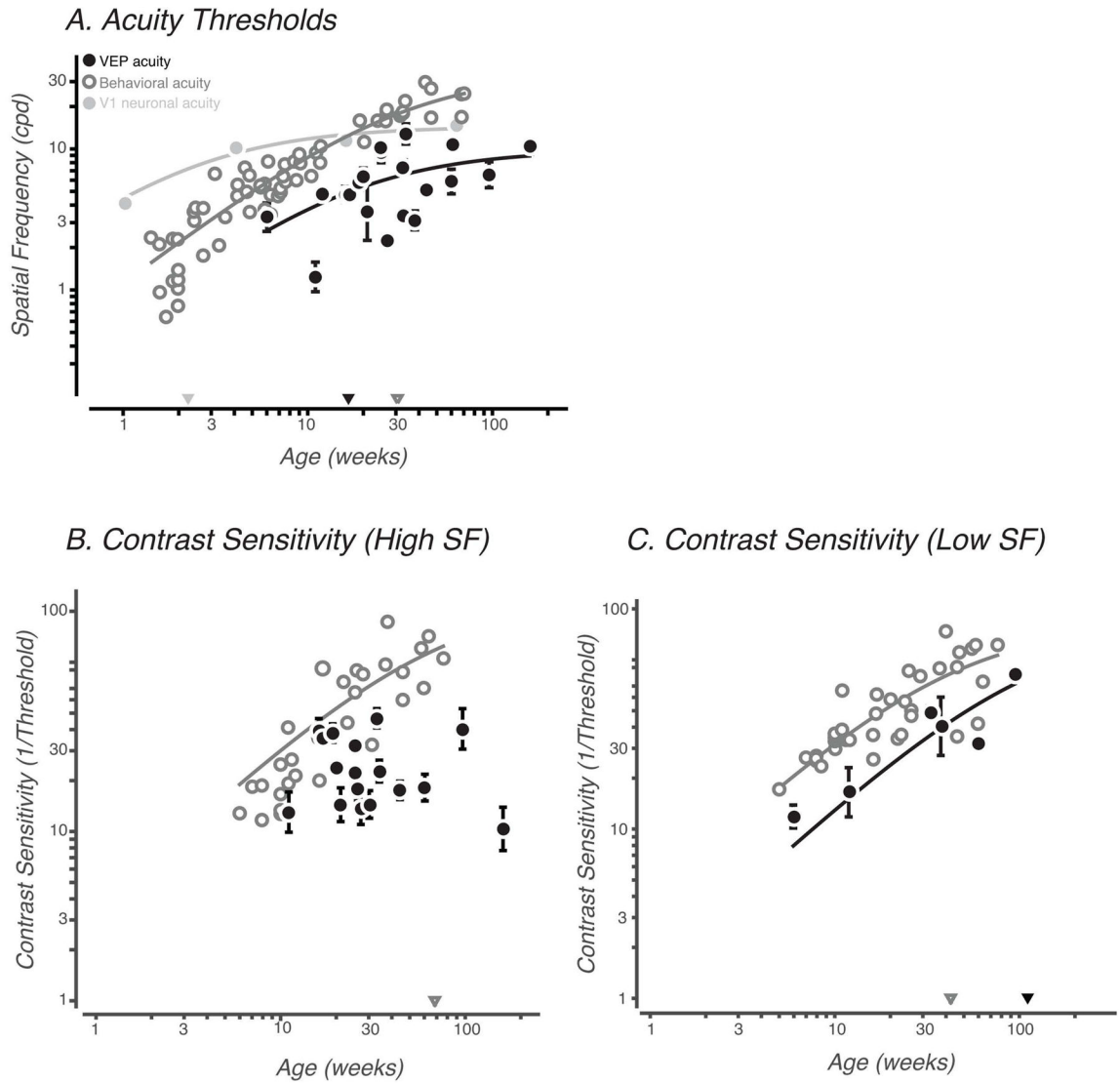
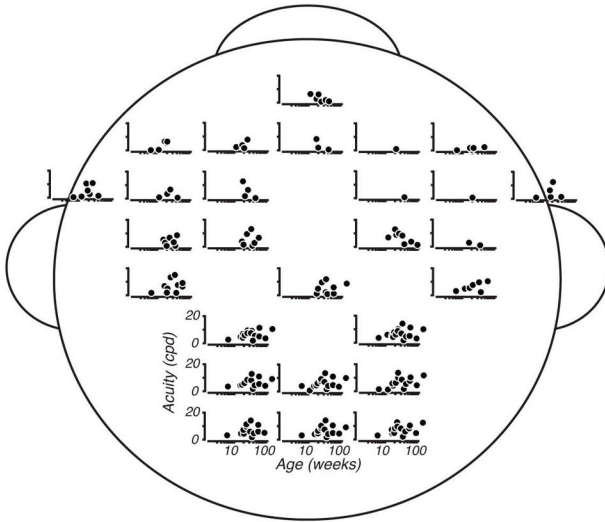
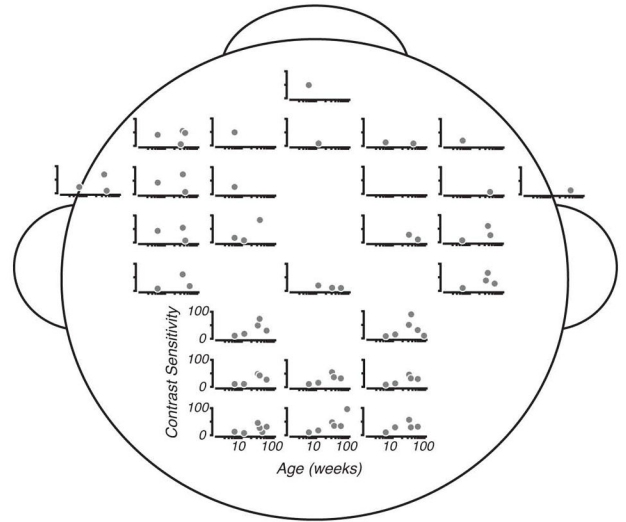


Figure 12. Longitudinal development of acuity (A) and contrast sensitivity (B–C) for three different measures: VEP (filled black circles), behavior (open grey circles) and neural recordings (filled grey circles). Developmental trajectories were captured by Michaelis-Menton fits, and evaluated for the age at which half-max thresholds were reached, when possible (arrows at the abscissa). VEP thresholds were evaluated using our new methods of threshold estimation; error bars represent the standard error. VEP-obtained thresholds were consistently higher than behavior.

A. Acuity Threshold



B. Contrast Sensitivity (Low SF)



C. Contrast Sensitivity (High SF)

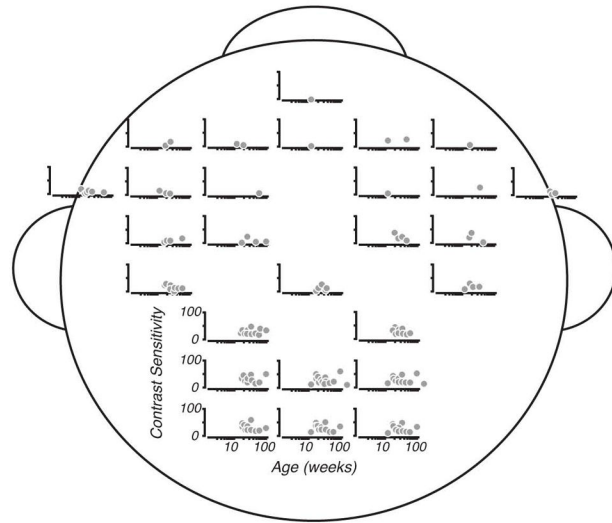


Figure 13. Longitudinal development of acuity (A) and contrast sensitivity (B–C) by electrode. Each sub-plot represents acuity or sensitivity as a function of age for the represented electrode position on the cap.

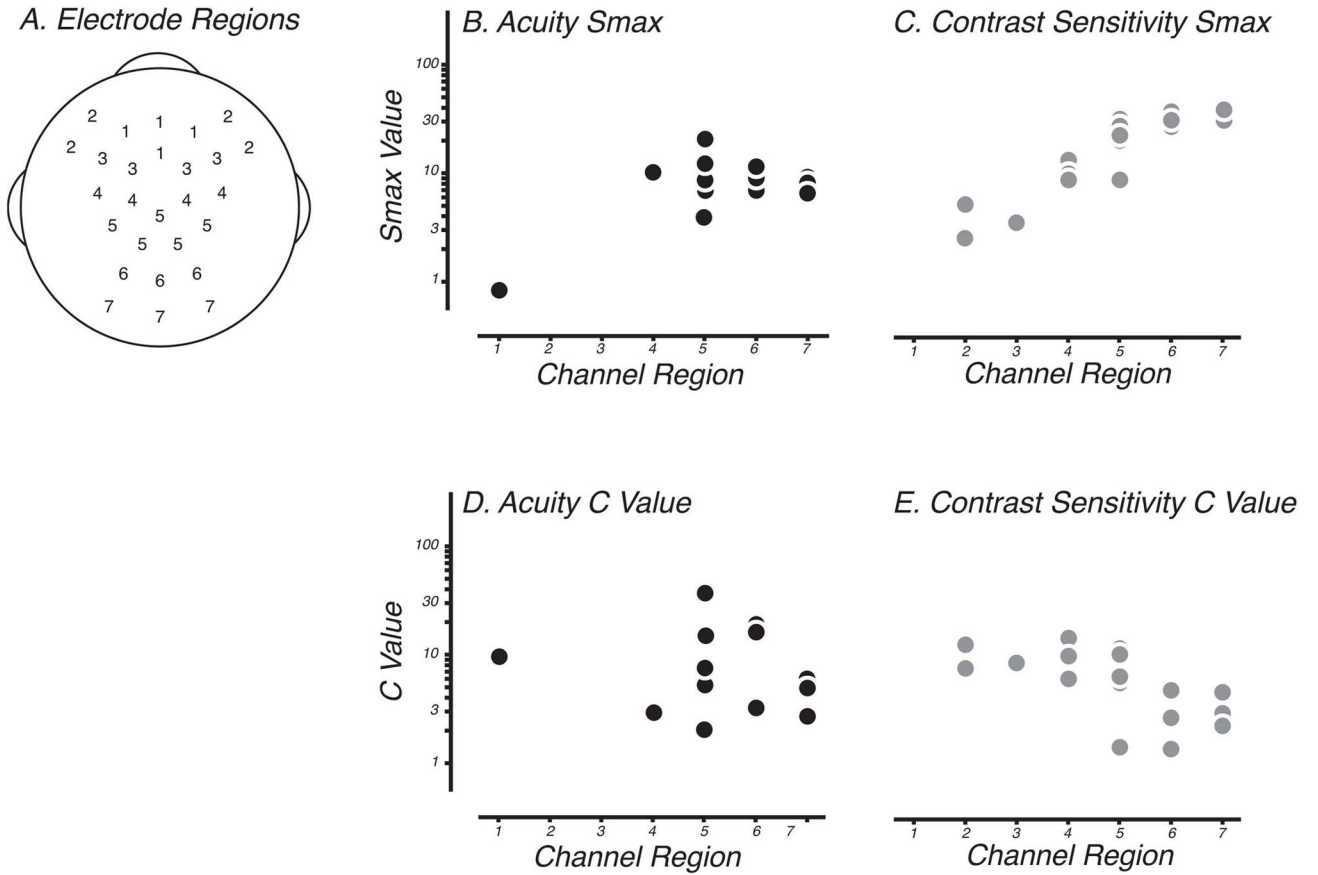


Figure 14. (A) Schematic of electrode regions on the cap. Each of the 27 electrodes was grouped into 1 of 7 spatial regions, over which developmental trajectories were analyzed. The longitudinal profile from a single animal was obtained for each electrode location and fit with a Michaelis-Menton function. From this fit, the resulting maximum sensitivity (Smax) (B–C) and age at which half maximum sensitivity (C) (D–E) was reached from that fit were then evaluated as a function of electrode region.